Biofilm 4 (2022) 100077

Contents lists available at ScienceDirect

Biofilm

journal homepage: www.sciencedirect.com/journal/biofilm

Sprayable biofilm – Agarose hydrogels as 3D matrix for enhanced productivity in bioelectrochemical systems

Melanie Tabea Knoll [a,b,1], Emely Fuderer [b], Johannes Gescher [a,b,*,1]

[a] Institute of Technical Microbiology, University of Technology Hamburg, Hamburg, Germany
[b] Karlsruhe Institute of Technology, Institute for Applied Biosciences – Department of Applied Biology, Karlsruhe, Germany

ARTICLE INFO

Keywords:
Microbiology
Biofilms
Shewanella oneidensis
Bioelectrochemical systems
Hydrogel
Sprayed biofilm

ABSTRACT

Bio-based energy production utilizing renewable resources can be realized by exoelectrogenic organisms and their application in bioelectrochemical systems (BES). These organisms catalyze the direct conversion of chemical into electrical energy and are already widely used in bioelectronics and biosensing. However, the biofilm-electrode interaction is a factor that limits sufficient space-time-yields for industrial applications. In this study, a hydrogel matrix consisting of agarose fibers was utilized as a scaffold for *S. oneidensis* cells to improve anodic processes in BES. This synthetic, scalable biofilm reached a higher current density in BES in comparison to naturally formed biofilms. Complemented with carbon nanofibers and riboflavin, the application of this functionalized hydrogel containing *S. oneidensis* cells led to an overall 9.1-fold increase in current density to 1324 mA m^{-2} in comparison to 145 mA m^{-2} for the planktonic control. In addition, the synthetic biofilm can be applied by spraying onto surfaces using a novel spray applicator. The latter allows to apply the biofilm effortless on large surfaces which will facilitate scalability and thus industrial application.

1. Introduction

A shift towards a bio-based economy is on-going and several new sustainable technologies were developed in this regard. One of these technologies focuses on the application of exoelectrogenic organisms such as *Shewanella oneidensis* in bioelectrochemical systems (BES) [1,2]. The latter can be used for bioenergy as well as platform chemical production. In these systems, microorganisms can act as a biocatalyst either on the anode to convert chemical substrates into electrical energy or on the cathode for bioelectrosynthesis purposes. Either way, the interaction of these organisms with the electrode surface is crucial for optimizing space-time-yields of these systems and to render them economically viable on an industrial scale. Microbe-electrode electron transfer can be catalyzed through direct contact of the organisms with the electrode or indirectly using endo- or exogenic electron shuttling molecules [3]. For an efficient direct electron transfer, the organisms colonize the electrode surface in the form of a biofilm. Efficiency is limited here by the ability to connect as many cells as possible to the electrode while minimizing diffusion limitation for substrates and products. For many organisms, including *S. oneidensis*, the naturally formed biofilms on electrodes are rather thin [4] and thus, productivity is limited. *S. oneidensis* is a BES model organism that has widely been studied regarding electrode-assisted fermentation, biosensing as well as wastewater treatment [2,5,6]. Besides its role as a model organism for exoelectrogenic electron transfer, the naturally formed biofilm of *S. oneidensis* cells is characterized by a comparatively low conductivity compared to other organisms utilized in bioelectrochemical processes [7]. Therefore, to improve direct electron transfer as well as biofilm formation in *S. oneidensis*, approaches for genetically engineering of the organism [8,9] as well as engineering the interface between electrode and bacteria [10–13] have been investigated. Regarding the latter approach, the use of biosurfactants for improving the biofilm-electrode-interaction has been studied [14]. For example, Zhang et al. could show that that anodic biofilm coverage could be almost 100-fold increased by adding rhamnolipids to the electrolyte of a BES system [15]. As another approach, synthetic tailor-made biofilms, in which the cells are embedded in a user-defined hydrogel, have become of interest. To this end, an artificial structure similar to the natural biofilm matrix that is produced over several days to months [16] can be provided immediately. Consequently, there are recent studies on synthetic biofilms investigating productive microorganisms embedded in hydrogel scaffolds. For example, Hu et al. embedded *S. oneidensis* cells in a nanocomposite,

* Corresponding author. Institute of Technical Microbiology, University of Technology Hamburg, Hamburg, Germany.
E-mail address: johannes.gescher@tuhh.de (J. Gescher).
[1] present address: Institute of Technical Microbiology, University of Technology Hamburg, Hamburg.

https://doi.org/10.1016/j.biofilm.2022.100077
Received 12 January 2022; Received in revised form 29 April 2022; Accepted 9 May 2022
Available online 18 May 2022

conductive DNA hydrogel that contained carbon nanotubes and silica nanoparticles to improve growth efficiency [11]. A functional bioanode consisting of alginate hydrogel and *S. oneidensis* was even shown to be printable with a reservoir-based 3D printer [12]. Furthermore, embedding *S. oneidensis* in PEDOT:PSS gels led to a 20-fold increase in current density compared to native biofilms in the first 18 h [17]. However, the production process of most analyzed hydrogels includes toxic monomers [17] or complicated manufacturing and application procedures [11,12] which hampers industrial applications. Combining scalablility and biocompatibilty, agarose hydrogels offer a convenient solution for this problem. This type of hydrogel has already been used to study the mechanical interactions between bacteria and their synthetic scaffold [18]. Other than the study by Suravaram et al., where a modified agarose hydrogel with embedded gold nanoparticles was used to increase the anode surface in BES, agarose hydrogels for enhanced bacteria-electrode-interaction have not yet been implemented for industrial usage or even electricity production. Suravaram et al. inoculated the system with planktonic *S. oneidensis* cells and the developed technology led to a 10-fold increase in current density after 24 h in comparison to an electrode without hydrogel [19]. This approach, however, led foremost to an increase in electrode surface area and, to our knowledge, synthetic biofilms formed by embedding exoelectrogenic cells into an agarose scaffold have not yet been investigated.

In this study, a hydrogel formed by non-modified low melt agarose was utilized as a 3D matrix for a synthetic *S. oneidensis* biofilm. The organisms were directly embedded in the hydrogel and current density in BES was used to assess process efficiency. Furthermore, two convenient application methods were developed in which the synthetic biofilm is introduced either by pouring or spraying. The possibility to spray the synthetic biofilm allows an enhanced scalabilty of the technique and consequently, will simplify implementation on an industrial scale. Different cell densities as well as gel heights were analyzed and the motility of the cells was investigated using fluorescence microscopy. Additionally, two additives were tested to prove the possibility of performance increase by tailoring the matrix to the specific needs of the process.

2. Materials and methods

2.1. Growth conditions and strains

All BES experiments were conducted with *S. oneidensis* MR-1 wild-type [20] except for the analysis of the cell distribution within the gel over 48 h. Here, a strain that expresses RFP was used for fluorescence microscopy [11]. Both strains were pre-cultured at 30 °C in LB media under oxic conditions. For the cultivation in BES an anoxic medium containing 20 mM lactate as electron donor was used. Furthermore, this medium contained per liter: 1.8 g $NaHCO_3$, 0.5 g Na_2CO_3, 0.2 g $MgCl_2$ x 6 H_2O, 1.0 mL selenite-tungstate solution (0.5 g L^{-1} NaOH, 3.0 mg L^{-1} Na_2SeO_3, 4.0 mg L^{-1} Na_2WO_4) and 100 mL salt solution (4.2 g L^{-1} KH_2PO_4, 2.2 g L^{-1} K_2HPO_4, 2.0 g L^{-1} NH_4Cl, 3.8 g L^{-1} KCl, 3.6 g L^{-1} NaCl). The medium was further complemented with 10.0 mL L^{-1} NB trace mineral solution [21], 10.0 mL L^{-1} vitamin solution (German Type Culture Collection, DMSZ, media 141), 0.2 mM sodium ascorbate, 0.4 mM $CaCl_2$ and 0.1% (w/v) yeast extract. The pH of the media was adjusted to 7.0 and oxygen was removed by flushing with N_2. Before inoculation of the BES, the cells were harvested by centrifugation (10 min, 6000 g) and washed twice with 1:10 diluted salt solution (see above). Cells were resuspended in 1:10 diluted salt solution. The RFP-expressing strain was cultivated with the addition of kanamycin (50 μg L^{-1}) and arabinose (1 mM) for plasmid maintenance and RFP expression, respectively.

2.2. Bioelectrochemical setup and chronoamperometric measurements

A three-electrode setup was used as BES with a working volume of 250 mL (Fig. 1). Graphite felt with a projected area of 16 cm^2 (4 cm × 4 cm of GFD 2.5, SGL Group, Germany) was used as the anode material with a BET (Brunauer-Emmet-Teller method) surface area of 0.4 m^2 g^{-1} and an area weight of 250 g m^{-2} (according to manufacturer). With this, the real surface area was calculated as 0.16 m^2, however, for current normalization the projected area of 16 cm^2 was used to compare the data to other current densities measured in comparable systems in literature [2,22–24]. Further, mean current density was calculated according to the following formula whereas I is the measured current and t is the time after which the experiment was stopped (24 h).

$$mean\ current\ density = \frac{\int_0^t I\,dt}{t}$$

Current data without normalization can be obtained from the supplementary information. As cathode a platinum gauze with a projected area of 1.25 cm^2 (1024 mesh cm^{-2}, 0.06 mm wire diameter, chemPUR, Germany) was used. An Ag/AgCl reference electrode (Sensortechnik Meinsberg, Germany) was used to adjust the working electrode potential during chronoamperometric measurements to −0.199 V vs. Ag/AgCl which relates to 0 mV against normal hydrogen electrode (NHE). A schematic drawing of the cell design is displayed in Fig. 1. Before use, the anode felt was rinsed with 2-propanol, followed by deionized water and the whole setup was sterilized by autoclaving. The system was constantly flushed with N_2 to provide anoxic conditions and the current was monitored for 24 h. All experiments were performed in triplicates. If stated, statistical significance was determined using an unpaired *t*-test with a p-value < 0.05.

2.3. Synthesis of agarose biofilms including addition of enhancing supplements

The synthetic biofilm consisted of *S. oneidensis* cells embedded in a low melt agarose hydrogel. For this, 1.8% (w/v) low melt agarose was prepared which was sterilized by autoclaving. The cells were precultured and washed as described above. Cell densities were calculated using a spectrophotometer measuring optical density at 600 nm. To this end we correlated optical density values with cell densities using correlation experiments conducted with a counting chamber (see below). The obtained cell densitiy values were extrapolated to the working volume of the bioelectrochemical cell of 250 mL. The prepared agarose solution was liquified by heating it to 90 °C and brought to 37 °C before the corresponding amount of cell suspension was added to the liquid agarose solution. The still liquid mixture was applied onto the working electrode by either pouring it into the mold or spraying it with the applicator (Fig. 3, a) onto the electrode. After not more than 1 min, the agarose hydrogel with embedded cells had solidified and the current production could be monitored using the bioelectrochemical setup described above. For the planktonic control, cells where directly added to the medium in the same number as described for the synthetic biofilm experiments. Moreover, we conducted a control in which an equal cell number without agarose was sprayed onto the anode material to elucidate the effect of simple direct application to the anode material compared to the addition as synthetic biofilm (figure S4). Riboflavin was added to the 37 °C liquid hydrogel in a concentration of 1.85 μM according to Arinda et al. [22] and cells were added afterwards as describe above. For the addition of 0.2% (w/v) carbon nanofibers (CNFs) the CNFs needed to be hydrophilized. For this, 2-propanol was added to the corresponding amount of CNFs and the mixture was treated in the ultrasonic bath for 10 min. Before the CNFs were functionalized with riboflavin, 2-propanol was evaporated at 80 °C for about 1 h. The dried CNFs were then resuspended in 7.4 μM riboflavin solution and sonified for 1 h at room temperature [25]. This CNF-riboflavin solution was diluted when adding it to the cell agarose suspension to a final riboflavin concentration of 1.85 μM. Both optimized synthetic biofilms were sprayed in the same manner as described above. Conductivity of the modified hydrogels was measured as described in the supplementary

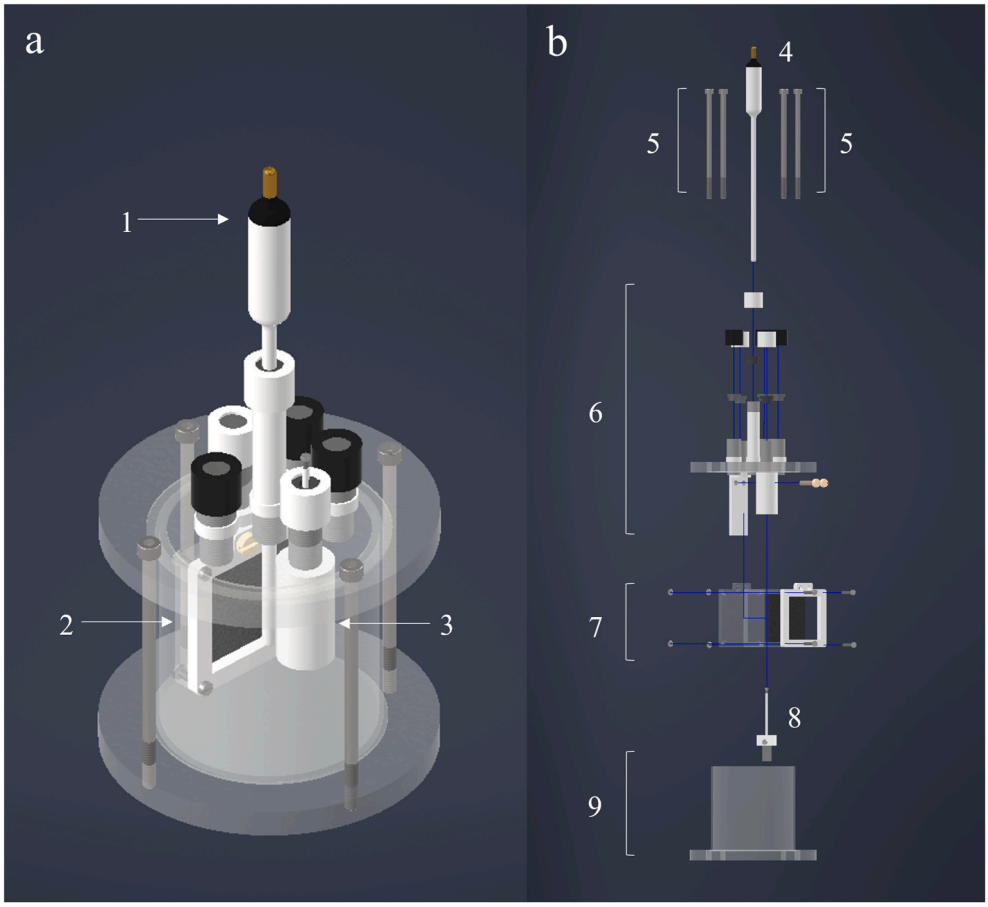

Fig. 1. Design of the bioelectrochemical reactor used in this study. (a) Reactor with 1) Ag/AgCl reference electrode, 2) fixture of anode material, graphite felt with projected area of 20 cm^2 and 3) fixture of cathode, platinum mesh with projected area of 1.25 cm^2. (b) Explosion graphic from bioelectrochemical cell. 4) reference electrode, 5) screws, 6) lid with holder for anode and cathode electrode including multiple ports for sampling and gas supply, 7) anode fixture, 8) cathode, 9) bottom and beaker, holding 250 mL cultivation medium.

information.

3. Calculation of cell number related to optical density

S. oneidensis wild type strain was cultivated in LB media over night at 30 °C. The cells were harvested by centrifugation as described above. The optical density (OD_{600}) of the suspension was adjusted to 0.5 and a Neubauer counting chamber was used to count the cell number per ml. The optical density of 0.5 equaled a cell concentration of 1.28×10^6 cells per ml. The cell number per ml gel was adjusted to five different cell densities for the characterization of current density and was kept at 3.98×10^7 cells per mL gel for all other experiments except the migration behavior experiment.

3.1. Migration behavior of embedded S. oneidensis cells within the hydrogel

A RFP-tagged strain [11] was used for the analysis of migration behavior of *S. oneidensis* cells embedded in agarose hydrogels. The fluorescence signal was utilized to characterize the distribution of cells in the gel after 0 h, 24 h and 48 h. The *S. oneidensis* hydrogel was poured onto the graphite felt electrode as described above with 0.79×10^7 cells mL^{-1} gel^{-1}. After the corresponding time period the felt was dismounted from the electrode mold and cut using a scalpel (10 mm × 2 mm) to image a cross section via fluorescence microscopy. A Leica DM5500B microscope with a 630-fold magnification as well as the software LASAF version 2.6 and ImageJ 1.53c were used for imaging and image analysis.

3.2. Sample preparation for SEM

S. oneidensis MR-1 wildtype strain was pre-cultured at 30 °C in LB overnight under oxic conditions. The cells were harvested by centrifugation (10 min, 6000 g) and washed twice with PBS solution containing 8 g L^{-1} NaCl, 0.2 g L^{-1} KCl, 1.44 g L^{-1} Na_2HPO_4 and 0.24 g L^{-1} KH_2PO_4. Cells were resuspended in PBS solution to which 4% formaldehyde was added. After fixation for 1 h at 4 °C the cells were centrifuged as described above and washed twice with ddH_2O. The agarose hydrogel was prepared as described above and the cells were embedded in 37 °C tempered agarose solution to form a synthetic biofilm hydrogel with a cell density of 0.79×10^7 cells mL gel^{-1}.10 μl of liquid synthetic biofilm was put on a silicone wafer and the sample was kept at −80 °C for at least 1 h before freeze drying it at −80 °C overnight. Thereafter, the sample was coated and analyzed using a Scanning Electron Microscope Leo 1530.

4. Results

The synthetic biofilm, consisting of a 1.25–5 mm thick 1.8% (w/v) low melt agarose hydrogel and *S. oneidensis* cells, was applied to the anode of a three-electrode BES setup (Fig. 1) by pouring directly onto the electrode surface. In a first set of experiments, the cell density within the synthetic biofilm was varied from 0.79×10^7 to 7.98×10^7 cells mL^{-1} gel and current density was measured over the time course of 24 h. The mean current density improved from 89.9 mA m^{-2} at a cell number per ml gel of 0.79×10^7 to a maximum of 243.0 mA m^{-2} beginning at a cell number of 5.98×10^7 per mL gel (Fig. 2, a). The results reveal that a further increase of the cell concentration did not have a significant influence ($p > 0.05$) on current production. Using one defined cell concentration of 3.98×10^7 cells mL^{-1} the influence of the gel thickness on current density was examined as this could have a pronounced impact on mass transfer limitations. Although the overall number of cells applied to the electrode was reduced by decreasing the synthetic biofilm

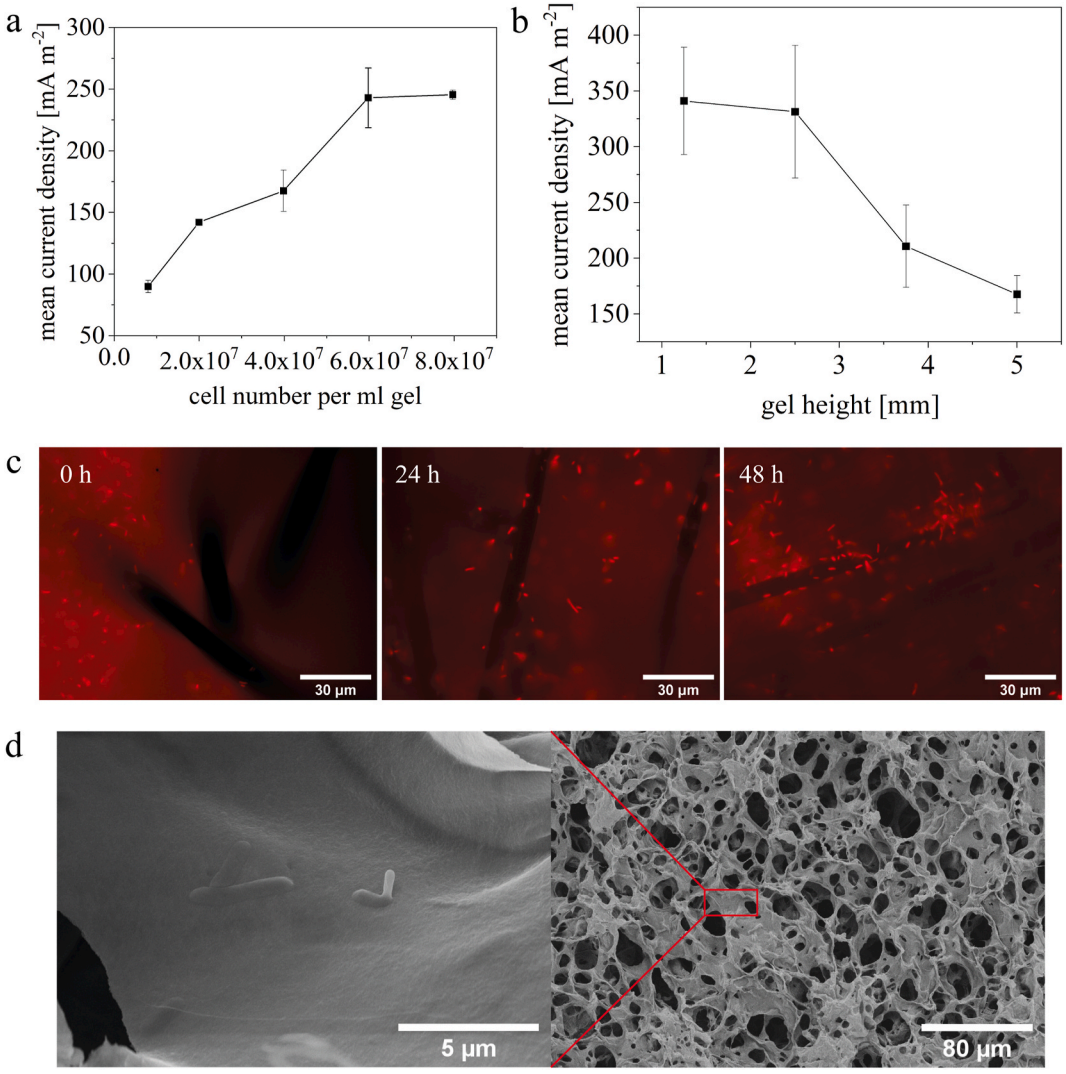

Fig. 2. Performance of synthetic *S. oneidensis* biofilms in bioelectrochemical systems (BES). Graphs display the average current density of independent triplicates over 24 h. The experiments were conducted in a three-electrode system with an applied potential of 0 V vs. NHE. (a) Correlation of cell concentration and current density. An increase of the cell number beyond 5.98×10^7 cells mL^{-1} did not lead to a significant increase in mean current density. (b) Biofilm heights were analyzed ranging from 1.25 mm to 5 mm. An increase in mean current density was achieved by reducing the biofilm height to 2.5 mm or below. (c) RFP-tagged *S. oneidensis* cells were analyzed within the hydrogel after 0 h, 24 h and 48 h. The images display the migration of the cells towards the graphite fibers. (d) SEM image of agarose hydrogel with embedded *S. oneidensis* cells.

height from 5 mm to 1.25 mm the current density increased from 167.6 to 341.1 mA m^{-2}. However, no significant difference between a 2.5- and 1.25-mm gel could be detected as both resulted in a current density of 331.4 ± 59.5 mA m^{-2} and 341.1 ± 48.3 mA m^{-2}, respectively.

Thereafter, it was investigated whether the localization of the cells within the synthetic biofilm matrix would be fixed after the agarose gel hardened. Hence, RFP-tagged *S. oneidensis* cells were embedded in a 5 mm thick agarose hydrogel and the overall cell distribution was analyzed after 0 h, 24 h and 48 h (Fig. 2, c). At 0 h the evenly distributed cells form a clear border between gel and graphite fibers. After 24 h and 48 h, respectively, cells accumulate onto the anodic electron acceptor. This accumulation of cells around the graphite fibers increased between 24 h and 48 h. We further gained insight into the 3D scaffold provided by the agarose hydrogel using scanning electron microscopy (Fig. 2, d). The formed 3D structure is visible as a network of micro channels with pores ranging from 10 to 40 µm in size.

As the pouring of the synthetic biofilm requires an electrode mold that can hold the liquid hydrogel until solidification, a more flexible application form was thought to be useful. To this end, as a second approach a spray application for the synthetic biofilm was developed. In this novel spray applicator (Fig. 3), the liquid synthetic biofilm is pushed via a syringe towards a Y-tube connector in which the hydrogel meets a continuous gas flow of N_2 and a spray mist is generated. This spray mist

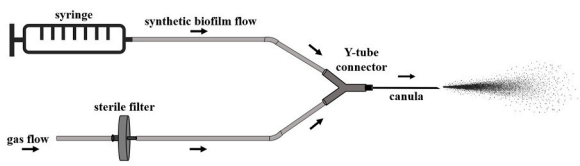

Fig. 3. Spray application of synthetic biofilm. (a) Design of spray applicator. The liquid bacteria hydrogel suspension in the syringe is pushed in the silicon tubing (outer Ø 3.5 mm) towards the Y-tube connector (for tube inner Ø 3.2 mm). Here, the liquid phase meets the gas flow (N_2) that is sterilized with a 0.2 µm filter and a spray mist is generated. The gas flow was provided via a gas bottle connected to a pressure regulator and 1 bar of pressure was used to generated the spray mist. The Y-tube is connected to the cannula (Ø 1.10 × 50 mm) via luer connector (inner Ø 3.2 mm). All parts of the applicator can vary in size as well as in diameter and making it therefore suitable for various applications.

is directed onto the graphite felt using a canula and current production of this sprayed, synthetic biofilm was analyzed.

The achievable current density using this sprayed biofilm containing 3.98×10^7 cells per mL gel was compared to a control to which the same number of cells was applied in the planktonic phase. In comparison with the planktonic control (Fig. 4, a) a performance improvement of 2.1-fold could be achieved within the first 24 h. This improvement is even more pronounced in the first 6 h with a 4.6-fold increase for the sprayed biofilm in comparison with the planktonic control with 226.3 mA m^{-2} and 49.0 mA m^{-2}, respectively. Additionally, this 2-fold improvement for the sprayed inoculation in comparison to the planktonic inoculation of cells was stable over a time period of 96 h (figure S5). The effects of spray inoculation were evaluated by spraying an equal cell number without the addition of agarose onto the anode which resulted in a current density of about 50 mA m^{-2} (figure S4). Comparing the two application procedures of pouring and spraying, both techniques led to a similar current density of 331.4 ± 59.5 mA m^{-2} for poured and 306.3 ± 58.0 mA m^{-2} for sprayed application if biofilms of similar height and same volume (4 mL) as well as identical cell concentration (3.98×10^7 cells per mL gel) were applied (Fig. 4, b). Furthermore, two additives were tested regarding their influence on current production. First, riboflavin, a soluble electron shuttle and cofactor of outer membrane cytochromes, was added to the gel in its liquid state and sprayed with the cells on the anode. The addition of riboflavin led to a 3-fold increase in current density, to a mean current density of 918.4 mA m^{-2}. The abiotic control consisting of a hydrogel with riboflavin but no cells showed no current production (figure S1). As riboflavin could be washed out from the biofilm matrix over time, we aimed for a stabilization of its position within the matrix and a further improvement of the biofilm properties by functionalizing carbon nanofibers (CNFs) with riboflavin [25] and homogenously distributing them within the matrix to increase the biofilm conductivity. The addition of activated riboflavin-CNFs resulted in a current density of 1324 mA m^{-2} which relates to a 4.3-fold increase in comparison to the synthetic biofilm without additives and a 9.1-fold increase compared to the planktonic control, respectively. Additionally, this riboflavin-CNF hydrogel resulted in the highest measured conductivity among the in this study modified agarose hydrogels (figure S3).

5. Discussion

A synthetic hydrogel consisting of *S. oneidensis* cells embedded in an agarose hydrogel was analyzed regarding its performance in BES. Agarose hydrogels have already been applied as a model for extracellular matrices of biofilms [13,18]. However, application for productive, synthetic biofilms has not yet been studied. To gain insight into the characteristics of this living biomaterial, cell density, gel thickness, motility of the cells in the BES system as well as the 3D matrix provided by agarose hydrogels was first investigated using the poured application form. For cell density a maximum in current density improvement was achieved at a cell concentration of 5.98×10^7 cells per ml gel. At that point a plateau in current production is reached as more cells did not result in a higher produced current density. When the same cell density is applied in different gel heights a lower gel height results in a higher current density. This is most likely due to the reduction of the diffusion barrier of the synthetic biofilm. It has already been shown for naturally formed biofilms that microniches are created by limiting diffusion of nutrients and that those result in a heterogeneous growth of the organisms within the biofilm matrix [26,27]. Stewart described diffusion in biofilms mathematically and postulated that biofilm thickness is proportional to diffusive penetration time [28]. Thus, by lowering the height of the synthetic scaffold the diffusion barrier was lowered as well. However, reducing the gel height below 2.5 mm was not accompanied anymore with a current density increase. Apparently, at this point mass transfer limitation was replaced by the number of current producing cells as limiting factor. Besides the reduction of the diffusion barrier, electron transfer could be influenced by the reduced gel height as well due to a lower resistance within the gel based on shorter distances and optimized cell distribution. Additionally, there are studies on lowering the energy density of bioelectrochemical systems by using smaller

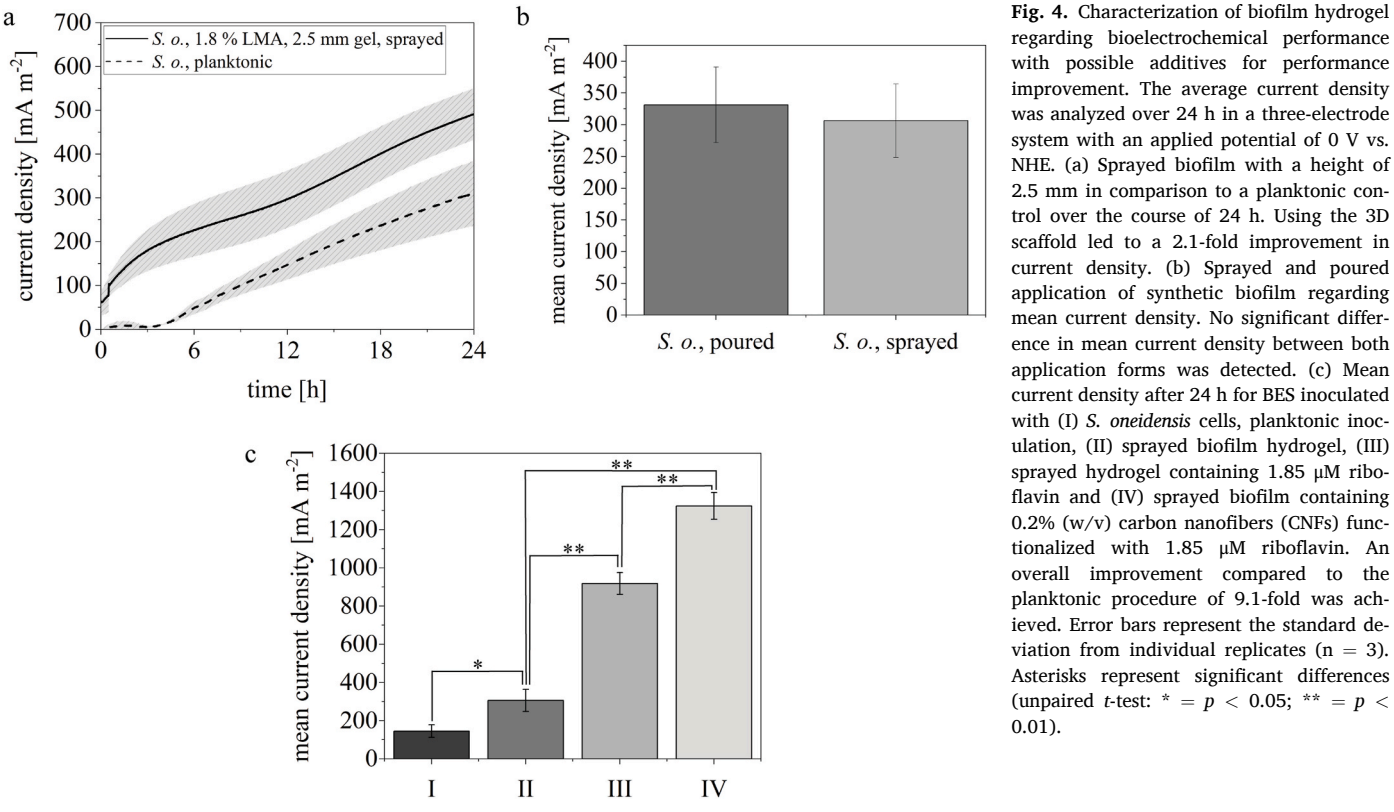

Fig. 4. Characterization of biofilm hydrogel regarding bioelectrochemical performance with possible additives for performance improvement. The average current density was analyzed over 24 h in a three-electrode system with an applied potential of 0 V vs. NHE. (a) Sprayed biofilm with a height of 2.5 mm in comparison to a planktonic control over the course of 24 h. Using the 3D scaffold led to a 2.1-fold improvement in current density. (b) Sprayed and poured application of synthetic biofilm regarding mean current density. No significant difference in mean current density between both application forms was detected. (c) Mean current density after 24 h for BES inoculated with (I) *S. oneidensis* cells, planktonic inoculation, (II) sprayed biofilm hydrogel, (III) sprayed hydrogel containing 1.85 μM riboflavin and (IV) sprayed biofilm containing 0.2% (w/v) carbon nanofibers (CNFs) functionalized with 1.85 μM riboflavin. An overall improvement compared to the planktonic procedure of 9.1-fold was achieved. Error bars represent the standard deviation from individual replicates (n = 3). Asterisks represent significant differences (unpaired *t*-test: * = $p < 0.05$; ** = $p < 0.01$).

reactor. For example, Ringeisen et al. reported that by increasing the surface area to volume ratio in their utilized mini-MFC that short diffusion lengths led to power outputs similar to the maxima known in literature [29]. A current density of about 20 mA m^{-2} for graphite felt was measured in this system which referred to a total current of about 1.25 mA. In the here presented study, the sprayed hydrogel biofilm without additives led to a total current of 0.49 mA and 2.12 mA with the addition of riboflavin-CNFs, respectively (table S1). Both systems follow a comparable optimization strategy and the here presented hydrogel/bacteria hybrid material could be an interesting addition to those miniature systems to further improve current production. Studying cell motility within the synthetic biofilm revealed that cell migration and/or cell proliferation within the hydrogel occurs at least over the time course of 48 h. Hence, although synthetically distributed in the beginning, the developed method allowed for further self-optimization of the catalytic process via positioning of the cells within the stable gradients of electron donor and carbon source availability. Examination of the synthetic biofilm via SEM analysis revealed pore sizes ranging from 10 to 40 μm (Fig. 2, d) which agrees well with other studies in which agarose was chosen as extracellular matrix model for studying biofilms as the pore sizes of 10–80 μm correlate well with the pore size of natural biofilms [13]. Hence, addition of a concentrated cell suspension did not affect the physical properties of the agarose and the channel structure remained unblocked which has a significant impact on diffusibility of the material. Since the physical accessibility of the synthetic biofilm is comparable to natural biofilms, these results illustrate the integrability of our novel synthetic materials in already existing industrial biofilm processes.

Subsequently, the spray applicator was used to offer an even more flexible application form, thus, producing a sprayable, productive biofilm. The 2.1-fold improvement compared to the planktonic inoculation highlights that the spatial fixation of the organisms directly onto the electrode comes with a significant increase in current production. Besides the designed direct interaction of cells with the electrode, we hypothesize that another factor could be involved as well in the current density increase. *S. oneidensis* cells entrapped in biofilm mimicking 3D scaffolds were shown to exhibit a reduced production of extracellular polymeric substances (EPS) involved in biofilm formation [30]. Xiao et al. showed that the depletion of EPS caused enhanced current production, most likely by higher interaction of c-type cytochromes with the electrode [31]. By providing a 3D scaffold, the gel matrix could inhibit the production of proteins relating to biofilm formation which results in an increased accessibility of c-type cytochromes and a consequently improved current production. Additionally, a higher metabolic energy demand by cells embedded in biofilm mimics has been shown for *S. oneidensis* embedded in alginate hydrogels which could relate to an enhanced performance due to a higher respiration rate [30].

We report here, for the first time, a spray application for synthetic, exoelectrogenic biofilms. Due to the utilization of standard laboratory equipment, our synthetic biofilm spray applicator allows a maximum of flexibility in the application of synthetic biofilms. For industrial application, scalability as well as robustness of this technique are indispensable. Those criteria are met by the herewith developed method. Additionally, we used low melt agarose to further lower the heat damage that has been described for bacterial cells during encapsulation in a agarose scaffold [13]. Further, both described application techniques resulted in comparable current densities. Therefore, we could reveal that the cells as well as their productivity were not negatively influenced during the spraying process in the presence of the hydrogel scaffold (figure S4). An additional control experiment, in which the spray inoculation was performed without agarose, showed that current density for sprayed cells without the hydrogel scaffold is even lower than the planktonic control as well as the sprayed hydrogel (figure S4). Therefore, the 3D matrix provided by the agarose hydrogel is directly related to the increased current density and the effect is not based on the local improvement in cell density but rather the mechanic properties of the hydrogel itself.

The addition of riboflavin and CNFs functionalized with riboflavin for current improvement showed the flexibility with which the synthetic scaffold can be functionalized to meet user-defined characteristics. The positive impact of riboflavin addition to BES has already been shown [32] but at least continuous processes suffer from a constant loss of this expensive compound from the fermentation broth [22]. The embedding of riboflavin into the hydrogel biofilm provides a method to immobilize it in spatial proximity to the exoelectrogenic cells. Regarding the immobilization of riboflavin near the electrode, the functionalization of CNFs with riboflavin displays that same effect. As for the effect of CNFs added to the 3D scaffold, Sanchez et al. showed that decreasing the diameter of the electrode material from microscale to nanoscale is beneficial solely because the created scaffold is more suitable for biofilm formation of *S. oneidensis* [33]. By adding of CNFs to the 3D scaffold of agarose, nanoscale CNFs within the microscale polymeric fibers are provided for colonization which could have a positive impact on current production. Further, conductivity measurements of the modified hydrogels showed an improvement in conductivity of the hydrogel with the addition of riboflavin-CNFs (figure S3). Therefore, electron transfer within the hydrogel could be improved due to higher conductivity which resulted in the shown increase in current density. Prospectively, this technology offers new opportunities to produce a ready-to-use synthetic biofilms that can be sprayed onto diverse types and sizes of electrodes. With the incorporation of conductive nanoparticles, the synthetic biofilm could even be applied as a fully functional 3D anode as it has been described in literature for *S. oneidensis* [12] with the possibility of spraying this biofilm on also semiconductive material still allowing electron transfer. When comparing the in this study achieved improvement provided by the hydrogel scaffold for the startup of BES, the achieved 9.1-fold increase is comparable with values from literature. As current production is highly depended on electrode surface as well as the used media, the improvement factor was used for comparison. For example, Lin et al. reported an increase in highest measured current of about 5-fold–20 μA after 6 h by embedding *S. oneidensis* in a phospholipid polymer in comparison to natural biofilms [34]. Yu et al. provided *S. oneidensis* cells with an matrix built by polypyrole and conductive micro-sized graphite and achieved an power density improvement of 11-fold in comparison with natural biofilms [35]. Further, Zajdel et al. used a PEDOT:PSS hydrogel matrix to increase current output 20-fold to a maximum current of 30 μA after 12 h [17]. The here reported 9.1-fold increase for the riboflavin-CNF spiked hydrogel with a total current of 2.12 mA after 24 h (table S1) is therefore in line with literature values while the fabrication and application technique offer an easier handling of the synthetic hydrogel/biofilm hybrid material. Furthermore, the utilization of this technique is not only limited to anodic processes but can also improve cathodic processes used for bioelectrosynthesis as well as biofilm-based gas fermentation. Consequently, following experiments will aim for the development of spray biofilms containing methanogens, acetogens or knallgas bacteria as biocatalysts and their application on cathodes in bioelectrochemical systems [36–38].

6. Conclusions

The here reported results reveal that spray application of tailor-made biofilms on electrodes has a significant impact on the performance of at least anodic bioelectrochemical processes. Additives for performance improvement led to an overall increase of current production of 9.1-fold in comparison to the planktonic control. The scalability and biocompatibility of this sprayable, synthetic biofilm allow for the implementation on an industrial scale. Nevertheless, not only *S. oneidensis* forms thin biofilms on electrodes. The same applies to for model organisms that are currently investigated for their applicability in bioelectrosynthesis, a process in which the organisms are supposed to grow on a cathode as electron and energy source. We hypothesize that similar positive effects can be achieved here as well which will be investigated in upcoming studies.

Declaration of interests

The authors declare the following financial interests/personal relationships which may be considered as potential competing interests.

Data availability

The data sets generated and analyzed during this study are shown in the manuscript or can be obtained from the corresponding author on reasonable request.

CRediT authorship contribution statement

Melanie Tabea Knoll: Conceptualization, Methodology, Validation, Formal analysis, Investigation, Writing, Visualization. **Emely Fuderer:** Investigation. **Johannes Gescher:** Conceptualization, Methodology, Validation, Writing, Visualization, Resources, Supervision, Project administration, Funding acquisition.

Declaration of competing interest

The authors declare that a patent application for sprayable, synthetic biofilm hydrogel (patent number 102021105164.9) has been filed. M.T. K. and J.G. are included in the patent and declare competing interest.

Acknowledgement

This work was financially supported from the project "Bioelectrochemical System for Flexible Biogas Production" of Fachagentur Nachwachsende Rohstoffe (grant number 2219NR051). We also thank Volker Zibat (LEM, KIT) for scanning electron microscopy analysis.

Appendix A. Supplementary data

Supplementary data to this article can be found online at https://doi.org/10.1016/j.bioflm.2022.100077.

References

[1] Zou L, Huang Y, Long Z, Qiao Y. On-going applications of Shewanella species in microbial electrochemical system for bioenergy, bioremediation and biosensing. World J Microbiol Biotechnol 2018;2018(351 35):1–9.
[2] Bursac T, Gralnick JA, Gescher J. Acetoin production via unbalanced fermentation in Shewanella oneidensis. Biotechnol Bioeng 2017;114:1283–9.
[3] Lovley DR. Electromicrobiology. Annu Rev Microbiol 2012;66:391–409.
[4] Biffinger JC, et al. Simultaneous analysis of physiological and electrical output changes in an operating microbial fuel cell with Shewanella oneidensis. Biotechnol Bioeng 2009;103:524–31.
[5] Simonte F, Sturm G, Gescher J, Sturm-Richter K. Extracellular electron transfer and biosensors. In: Advances in biochemical engineering/Biotechnology, 167 15–38. Springer Science and Business Media Deutschland GmbH; 2019.
[6] Logan BE, Rabaey K. Conversion of wastes into bioelectricity and chemicals by using microbial electrochemical technologies. Science (80-.) 2012;337:686–90.
[7] Malvankar NS, Lovley DR. Microbial nanowires: a new paradigm for biological electron transfer and bioelectronics. ChemSusChem 2012;5:1039.
[8] Joshi K, Kane AL, Kotloski NJ, Gralnick JA, Bond DR. Preventing hydrogen disposal increases electrode utilization efficiency by Shewanella oneidensis. Front Energy Res 2019:95. 0.
[9] Silva AV, Edel M, Gescher J, Paquete CM. Exploring the effects of bolA in biofilm formation and current generation by Shewanella oneidensis MR-1. Front Microbiol 2020:815. 0.
[10] Iannaci A, et al. Tailored glycosylated anode surfaces: addressing the exoelectrogen bacterial community via functional layers for microbial fuel cell applications. Bioelectrochemistry 2020;136:107621.
[11] Hu Y, Rehnlund D, Klein E, Gescher J, Niemeyer CM. Cultivation of exoelectrogenic bacteria in conductive DNA nanocomposite hydrogels yields a programmable biohybrid materials system. ACS Appl Mater Interfaces 2020;12:14806–13.
[12] Freyman MC, Kou T, Wang S, Li Y. 3D printing of living bacteria electrode. Nano Res 2020;13:1318–23.
[13] Strathmann M, Griebe T, Flemming H-C. Artificial biofilm model – a useful tool for biofilm research. Appl Microbiol Biotechnol 2000;2000(542 54):231–7.
[14] Pasternak G, Askitosari TD, Rosenbaum MA. Biosurfactants and synthetic surfactants in bioelectrochemical systems: a mini-review. Front Microbiol 2020;11:358.
[15] Zhang Y, et al. Accelerating anodic biofilms formation and electron transfer in microbial fuel cells: role of anionic biosurfactants and mechanism. Bioelectrochemistry 2017;117:48–56.
[16] Butti SK, et al. Microbial electrochemical technologies with the perspective of harnessing bioenergy: maneuvering towards upscaling. Renew Sustain Energy Rev 2016;53:462–76.
[17] Zajdel TJ, et al. PEDOT:PSS-based multilayer bacterial-composite films for bioelectronics. Sci Rep 2018;8:1–12.
[18] Kandemir N, Vollmer W, Jakubovics NS, Chen J. Mechanical interactions between bacteria and hydrogels. Sci Rep 2018;2018(81 8):1–11.
[19] Suravaram SK, Smith DK, Parkin A, Chechik V. Conductive gels based on modified agarose embedded with gold nanoparticles and their application as a conducting support for *Shewanella Oneidensis* MR-1. Chemelectrochem 2019;6:5876–9.
[20] Dolch KJJ. Genomic barcode-based analysis of exoelectrogens in wastewater biofilms grown on anode surfaces. J Microbiol Biotechnol 2016;26:511–20.
[21] Coppi MV, Leang C, Sandler SJ, Lovley DR. Development of a genetic system for geobacter sulfurreducens. Appl Environ Microbiol 2001;67:3180–7.
[22] Arinda T, et al. Addition of riboflavin-coupled magnetic beads increases current production in bioelectrochemical systems via the increased formation of anode-biofilms. Front Microbiol 2019;10:126.
[23] Chen W, et al. Enhancing performance of microbial fuel cells by using novel double-layer-capacitor-materials modified anodes. Int J Hydrogen Energy 2018;43:1816–23.
[24] Wang Y, Wen Q, Chen Y, Li W. Conductive polypyrrole-carboxymethyl cellulose-titanium nitride/carbon brush hydrogels as bioanodes for enhanced energy output in microbial fuel cells. Energy 2020;204:117942.
[25] Toshimitsu F, Ishimaru W, Nakashima N. Individual solubilization behavior of single-walled carbon nanotubes by riboflavin (Vitamin B2) in water and its analyses using regression approach and computational simulations. Chem. Soc. Japan 2019;92:1679–83.
[26] Xu KD, Stewart PS, Xia F, Huang CT, McFeters GA. Spatial physiological heterogeneity in Pseudomonas aeruginosa biofilm is determined by oxygen availability. Appl Environ Microbiol 1998;64:4035–9.
[27] Wentland EJ, Stewart PS, Huang CT, McFeters GA. Spatial variations in growth rate within Klebsiella pneumoniae colonies and biofilm. Biotechnol Prog 1996;12:316–21.
[28] Stewart PS. Diffusion in biofilms. J Bacteriol 2003;185:1485–91.
[29] Ringeisen BR, et al. High power density from a miniature microbial fuel cell using Shewanella oneidensis DSP10. Environ Sci Technol 2006;40:2629–34.
[30] Zhang Y, Ng CK, Cohen Y, Cao B. Cell growth and protein expression of Shewanella oneidensis in biofilms and hydrogel-entrapped cultures. Mol Biosyst 2014;10:1035–42.
[31] Xiao Y, et al. Extracellular polymeric substances are transient media for microbial extracellular electron transfer. Sci Adv 2017;3:e1700623.
[32] Marsili E, et al. Shewanella secretes flavins that mediate extracellular electron transfer. Proc Natl Acad Sci 2008;105:3968–73.
[33] Sanchez DVP, et al. Changes in carbon electrode morphology affect microbial fuel cell performance with Shewanella oneidensis MR-1. Energies 2015;8(8):1817–29. 1817–1829 (2015).
[34] Lin X, Nishio K, Konno T, Ishihara K. The effect of the encapsulation of bacteria in redox phospholipid polymer hydrogels on electron transfer efficiency in living cell-based devices. Biomaterials 2012;33:8221–7.
[35] Yu YY, Chen HL, Yong YC, Kim DH, Song H. Conductive artificial biofilm dramatically enhances bioelectricity production in Shewanella -inoculated microbial fuel cells. Chem Commun 2011;47:12825–7.
[36] Reiner JE, et al. From an extremophilic community to an electroautotrophic production strain: identifying a novel Knallgas bacterium as cathodic biofilm biocatalyst. ISME J 2020;2020(145 14):1125–40.
[37] Jung T, Hackbarth M, Horn H, Gescher J. Improving the cathodic biofilm growth capabilities of Kyrpidia spormannii EA-1 by undirected mutagenesis. Microorg 2020;9(77 9):77. 2021.
[38] Hackbarth M, et al. Monitoring and quantification of bioelectrochemical Kyrpidia spormannii biofilm development in a novel flow cell setup. Chem Eng J 2020;390:124604.